oC1

INVESTIGATION OF LASER-INDUCED PLASMA EMISSION FOR ZnO THIN FILM DEPOSITION

S. ABDELLI-MESSACI, T. KERDJA, S. LAFANE and S. LEMLIKCHI
Centre de Développement des Technologies Avancées,
Haouch-Oukil, B.P. 17, Baba Hassen, Algiers, Algeria
E-mail : messaci@cdta.dz

ABSTRACT: ZnO plasma emission was investigated by ICCD camera fast imaging and by time integrated optical emission spectroscopy into vacuum and oxygen ambience. The ZnO plasma was induced by a KrF excimer laser ablation of zinc oxide target. This experiment was carried out at different O_2 pressures from 10^{-2} to 10 *mbar*. Based on experimental findings by fast imaging, plume expansion as a function of ambient gas can be categorized into three different regimes, low ($< 10^{-2}$ *mbar*), intermediate ($10^{-2} < P < 1$ *mbar*) and high pressures (> 1 *mbar*). Each of these regimes is characterized by a particular behavior of plume dynamics; freely expansion, plume splitting and enhancement of intensity and hydrodynamic instability and shock-wave-like propagation of the plume.
The time integrated optical emission spectra acquired at a certain distance from the target into vacuum and for 0.1, 1 and 5 *mbar* oxygen pressures reveals several emission lines due to neutral zinc Zn*, zinc cation Zn^+* and oxygen atom O* but no feature attributable to excited oxygen cations were identified. By comparing time integrated optical spectrum of plasma taken at different distances, the emission intensity of Zn^+* line decreases as the distance from the target increases and disappears far from it.
Furthermore, ZnO thin films were deposited in the three different regimes of O_2 pressures used in order to correlate between plasma dynamics and deposited film characteristics.

KEYWORDS: laser ablation, fast imaging, laser induced plasma spectroscopy, zinc oxide

1. Introduction

The growth of thin films by pulsed laser deposition (PLD) is a process that depends on many factors, such as density, energy, ionization degrees and type of the condensing particles as well as the temperature and physicochemical properties of the substrate [1]. PLD technique has been largely used to deposit ZnO films. It is found that the characteristics of ZnO films are generally affected by the preparation conditions used in PLD such oxygen pressure, substrate temperature and substrate type. Zinc oxide nanocrystalline is considered as one of the most promising materials for optoelectronic devices such as UV light emitting (diodes, lasers) as well as electrodes in solar cells and in phosphor screens, sensors and surface acoustic wave devices [2]. Generally, the control of the laser induced plasma plume is achieved only with a good understanding of the basic physics and chemistry associated with laser-target and particle-particle interaction within the laser induced plasma plume.The plasma dynamics under reactive gas remains an interesting field to study in order to understand the complex physico-chemical mechanisms involved, including shockwaves, hydrodynamic instabilities and chemical reactions. These phenomena depend on gas pressure, laser parameters and focal spot size and shape [3]. The presence of the surrounding gas during expansion may also lead to reactive scattering, thermalization of the plume, enhanced condensation leading to cluster and nanoparticle formation [4].

In this work, we study the effect of oxygen pressure on both plasma dynamics during laser ablation of a zinc oxide target and on morphology and crystalline structure of deposited ZnO films.

2. Experimental setup

The schematic of the experimental setup is given in figure 1. The zinc oxide target was mounted onto a rotating holder inside a stainless steel vacuum chamber. The air in the latter was evacuated with a turbo-molecular pump to a residual pressure of 10^{-6} *mbar* and then filled with oxygen gas. A KrF excimer laser (Lambda Physik Compex 102) operating at 248 *nm* with pulse duration of 25 *ns* was focused through two cylindrical lenses (L1, L2), onto the target surface at an incidence angle of 45°. The spot size area is about 2 mm^2 and the laser fluence was set to 2 J/cm^2. The light emitted by the plume was observed along the direction perpendicular to the ejection through a fast intensified charge-coupled device (ICCD, Princeton Instruments PI-MAX, 1024 x 256 pixels, pixel size = 26 x 26 *µm*) with 5 *ns* minimum gate control. The detector consists of a micro channel plate (MCP) with spectral response of 190-850 *nm*. A programmable timing generator (PTG) was used to control the time delay between the laser pulse and the detector system. A set of spherical (SM) and planar (PM) mirrors and a 76 *mm* focal length objective (Zeiss) placed in front of the camera were used to image the plasma onto the detector surface with a magnification of 1/3.

Spectrally resolved measurements of the plasma emitted light were carried out by imaging a portion of plasma onto 50 *µm* entrance slit of a miniature spectrometer S2000 (Ocean Optics) with a spectral resolution of 3 *nm*. The collected light was transmitted by means of an optical fiber (see figure 1). The spectrometer is equipped with a no-gated detector high-sensitivity CCD linear array (Sonny ILX511) which is connected to a data acquisition.

Zinc oxide films were deposited on Si (001) substrates at different pressures from 2 10^{-2} to 5 *mbar*. The substrates were placed at a fixed distance of 30 *mm* from the target surface and their temperature was kept at 300°C. The structural properties of the films were characterized by X-ray diffraction (Bruker AXS: D8 ADVANCE). The surface morphology was investigated using a scanning electron microscopy (SEM-JEOL 6400).

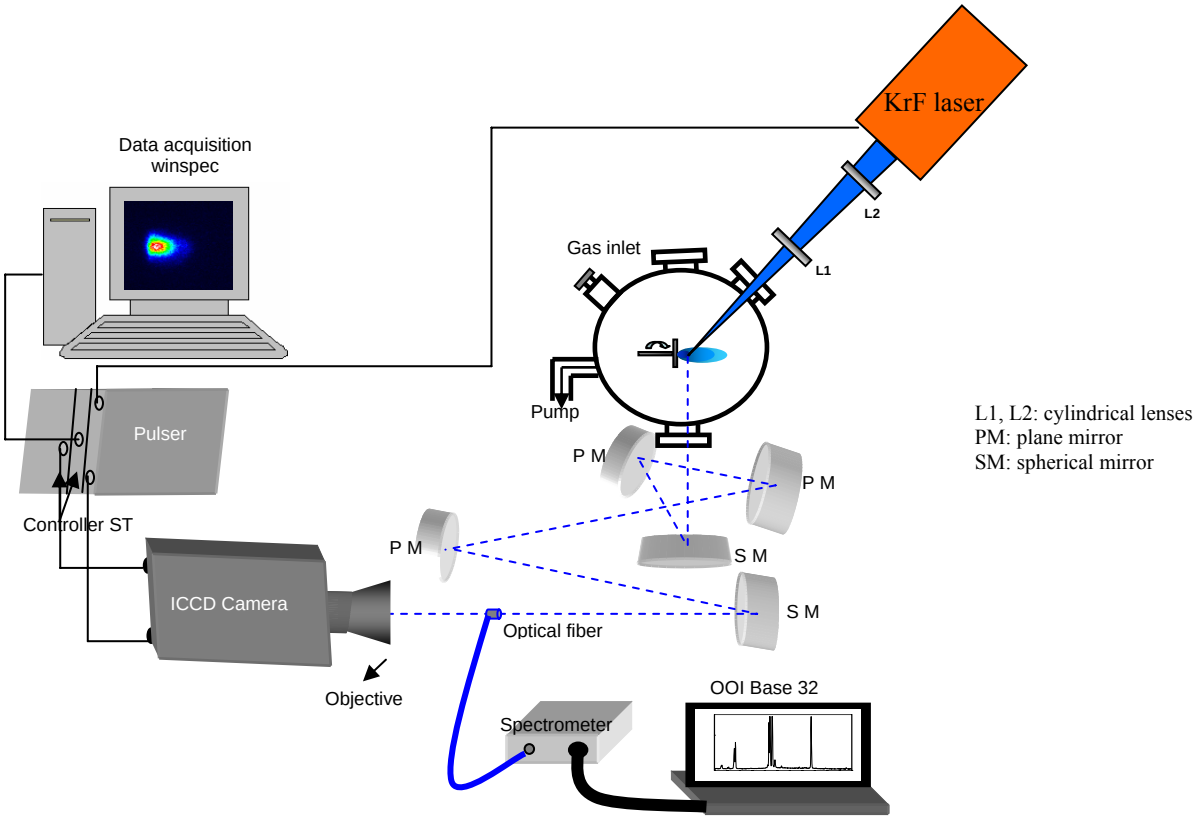

Figure 1: Schematic of the experimental setup

3. Results and discussion

3. 1. Fast imaging

Two-dimensional images of visible ZnO plasma emission recorded at different delay time following the laser pulse into vacuum and 1×10^{-2}, 5×10^{-1}, 1, 5 and 10 *mbar* oxygen pressures are reported in Figures 2. Images were recorded for either all visible emission within 350-800 *nm* (limited by the spectral windows of the objective). In vacuum the plasma expand freely without any friction. In presence of gas and at a pressure of 10^{-2} *mbar* the plasma expansion seems like in vacuum except at a delay time of 2 *µs* and more which undergo broadening. Therefore at 0.5 and 1 *mbar* O_2 pressures, several effects are observed, the stratification of plasma, a shock front formation and hydrodynamic instabilities apparition. These effects become pronounced as the pressure increases and as plasma species expand in time.

Based on experimental findings, plume expansion as a function of ambient gas can be categorized into three different regimes, low (< 10^{-2} *mbar*), intermediate (10^{-2} < P <1 *mbar*) and high pressures (> 1 *mba*r). Each of these regimes is characterized by a particular behavior of plume dynamics. At low pressures the plume expands freely without any external viscous force. At intermediate pressures, the effect of background gas on the expansion dynamics begins, resulting in the plume splitting and enhancement of intensity. At relatively high pressure, interpenetration of the plume species and background gas is relatively difficult. The plasma species pushes away the background gas. The compressed gas restricts any further expansion of the plume and confines it in a small volume. The expansion regime transforms into a hydrodynamic instability and shock-wave-like propagation of the plume [5, 6].
We notice that during the plasma expansion, instability attributed to Rayleigh Taylor (RT) is set in the contact boundary gas-plasma. The exponential growth of RT instability is given by e^{nt} at a rate :

$$n^2 = Ka\,(\rho_p - \rho_g)/(\rho_p + \rho_g) \qquad (1)$$

where ρ_p and ρ_g are the plasma and background gas densities, $a=dv/dt$ with v being the velocity of the plasma front and K the instable mode wave vector. The plasma front becomes instable when $\rho_p < \rho_g$. The instability growth occurs in the maximum acceleration region where it can be derived from the derivatives of the momentum conservation equation,

$$d/dt\,[(M_0 + 4/3\,\pi R^3\rho_g)v] = 0 \qquad (2)$$

where M_0 is the plasma mass. Then the critical density is given by $\rho_g = 3M_0/4\,\pi R^3$.
Using our experimental parameters, we have estimated the density of the background gas where the RT instability can form. The mass of the ablated material was calculated by the measure of target weight before and after ablation with 6000 laser shots and it was found to be 8 *µg/pulse*. Taking the experimentally observed distance d = 10 *mm*, the calculated density of the background gas ρ_g was 1.9 $\mu g/cm^3$ which correspond to a pressure of 1.34 *mbar*. This is in good agreement with our experimental observation that pressures ≥ 1 mbar correspond to the hydrodynamical regime for the expanding plume.

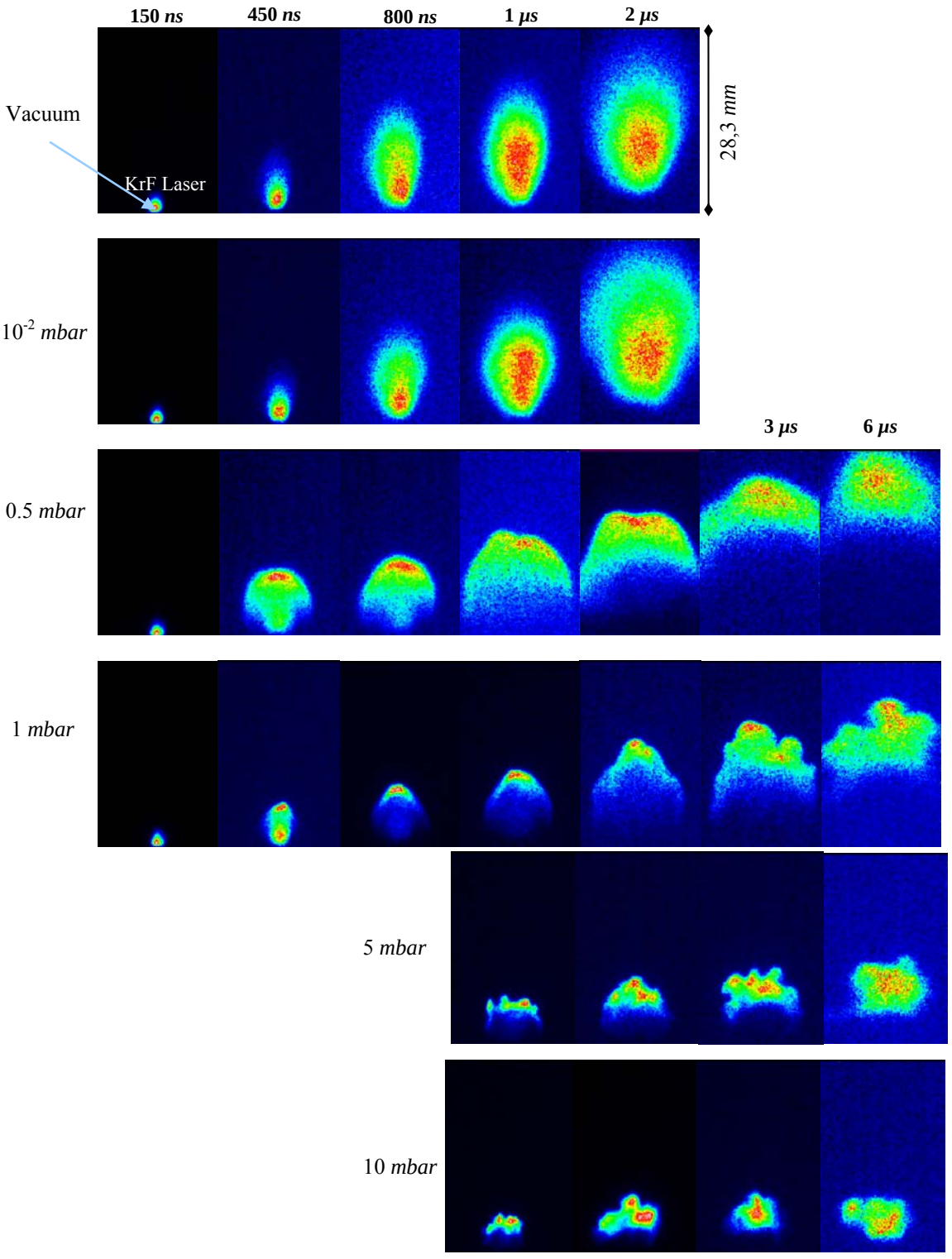

Figure 2 : Images of ZnO plasma emission recorded at different delay time following the laser pulse into vacuum and at different oxygen pressures 1×10^{-2}, 5×10^{-1}, 1, 5 and 10 *mbar*.

The effect of background gas on the expansion dynamics of the plasma front at 0.5, 1, 5 and 10 *mbar* O_2 pressures can also be observed in the distance-time (R-t) plots shown in figure 3. We notice a linear behavior indicative of a free expansion at the early stage of expansion and then the plume front gradually slows down and is more effective as O_2 pressure is raised. This slowing down start at a time delay greater than 1 *μs* at 0.5 and 1 *mbar* and 0.5 *μs* at 5 and 10 *mbar* and approaches a stationary behavior at larger times at 10 *mbar*. This marks the occurrence of plume stopping in the late stage of the plume expansion. This stopping is reached when the shock wave developed in the plasma front degenerates into a sound wave in the background gas [6,7]. The plume stopping indicates the transition from a hydrodynamic expansion of the plume to a diffusion-like propagation of the ablated species in the surrounding gas.

Moreover, we notice an oscillating behavior which is well distinct at 5 *mbar*. When the RT instability grows up, the position of the plasma front is not well defined and can lead to this oscillatory behavior. This latter can also be related to the formation of several reflected shocks within the plasma as it has been predicted by Bulgakov and Bulgakova [8] and Chen *et al*. [9].

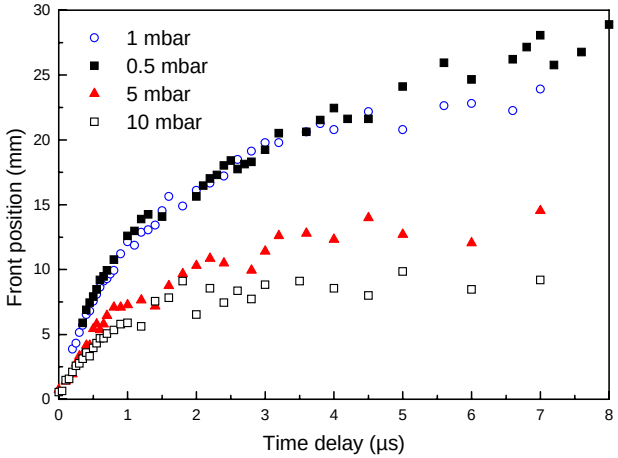

Figure 3: Distance versus time of the plasma front at 0.5, 1, 5 and 10 mbar O_2 pressures

3. 2. Time integrated optical emission spectroscopy

In order to have an idea of the emitted plasma species, time integrated emission spectrum of ZnO plasma has been recorded using optical emission spectroscopy (see figure 1). In figure 4 we report the time integrated optical emission spectra acquired at a distance (*d*) of 2.6 *mm* from the target into vacuum and for 0.1 and 5 mbar oxygen pressures. The spectra show several emission lines due to excited neutral zinc Zn (328.2, 334.5, 468, 472.2, 481, 636.2 *nm*), single ionized zinc Zn^+ (491.3 and 492.5 *nm*, the both lines are confused) and oxygen atom O (777.3 *nm*) but no feature attributable to excited oxygen cations O^+ were identified. The non-observation of oxygen cationic lines in the emission spectrum implies that the plume is not hot enough. The energy required for ionization of oxygen is 13.62 *eV* which is higher then the ionization potential of Zn (9.36 *eV*).

We notice that the emission lines of Zn^+ are emitted both into vacuum and oxygen pressure. Figure 5 shows the plasma emission spectra taken at different distances from the target 1.8, 2.6, 4.8 and 9 *mm* for 5 *mbar* O_2. However, some new features are observed by comparing time integrated optical spectra of plasma taken at different distances from the target for 0.1, 1 and 5 *mbar* O_2 pressures (only spectra recorded at 5 *mbar* O_2 are presented here). The

emission intensity of Zn^+ line decreases as the distance from the target increases and disappears far from it. This feature could result from a recombination process by electronic impact. Claeyssens *et al.* [10] have studied ArF laser ablation of ZnO target under vacuum by optical emission spectroscopy. They found that only Zn features are evident in the plasma spectrum emission recorded at lower fluence at a distance of 5 *mm*. Kawaguchi *et al.* [11] have found that the plasma emission provides only from Zn of laser ablation ZnO target at a fluence of 1.5 J/cm^2 into helium atmosphere at a distance of 30 *mm* from the target.

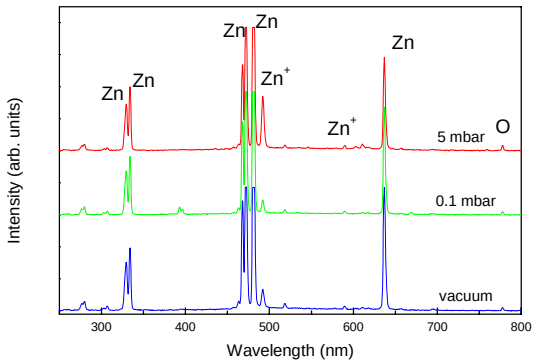

Figure 4 : Time integrated optical emission spectra acquired at d = 2.6 *mm* from the target in vacuum, 0.1 and 5 *mbar* oxygen pressures.

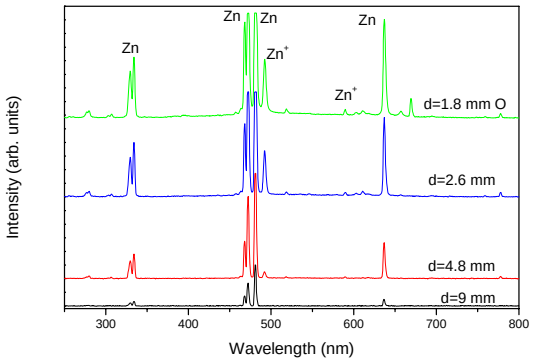

Figure 5 : Time integrated optical emission spectra recorded at different distances for 5 *mbar* oxygen pressure.

3. 3. ZnO films deposition

Figure 6 represents the XRD spectra of the ZnO films grown on Si (001) at various oxygen pressures. Each spectrum is normalized to its maximum peak intensity. According to XRD spectra, the film quality increases when oxygen pressure decreases. At high oxygen pressure, the grown films show random oriented structures which indicate low film crystallinity. However, at 0.02 *mbar*, the crystallinity is improved and the well c-axis oriented ZnO film is formed.

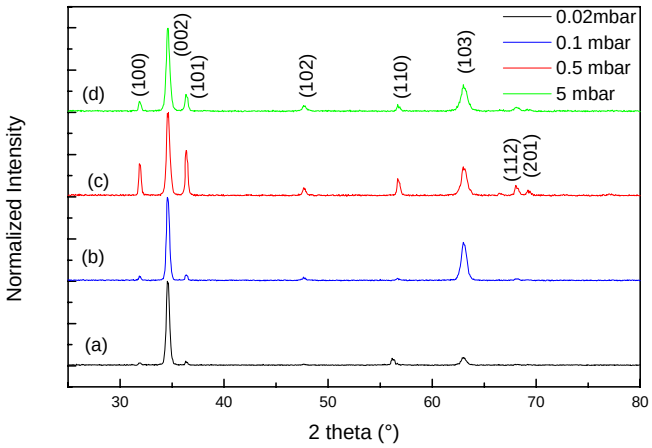

Figure 6: XRD patterns of ZnO films deposited at 0.02, 0.1, 0.5 and 5 *mbar* O_2 pressures

For a high crystallinity films, there must be sufficient time for adatoms to undergo surface diffusion to look for the lowest energy sites to reach thermodynamic stability before being covered by the next layer of atoms [12, 13]. The film crystallization is affected by the kinetics of atomic arrangements, depending on the substrate temperature and the deposited particles kinetic energy. The latter is controlled by the ambient gas pressure. By increasing the oxygen pressure, the kinetic energy of the ejected species decreases by collisions with the gas particles. The decrease in energy of atoms limits the possibility of adatoms to seek for the lowest energy position. In our case, for pressures (≥ 0.5 *mbar*) the target-substrate distance is larger then the plume stopping distance as we can see on figure 3. This indicates that the ablated species are thermalized before reaching the substrate leading to lower deposition energy. Consequently, the film crystallinity might be deteriorated.

Figure 7 shows the surface morphology of ZnO thin films carried out at 0.02, 0.1, 0.5 and 5 *mbar* oxygen pressures. At 0.02 *mbar* (fig. 7a), ZnO film exhibits honeycomb like structure with non uniform cell size. Figure 7b shows ZnO film deposited at 0.1 *mbar* oxygen pressure. The film exhibits a spaghetti-like structure with a grain diameter around 30nm. However, at 0.5 and 5 *mbar* surface morphology shows granular structure with different shape and size grains (see figures 7c and 7d). At low oxygen pressure, the ablated particles have sufficient kinetic energy to reach substrate surface. They can look for the lowest energy sites, agglomerate, and then nucleate together. For the honeycomb structure, the ZnO islands are formed onto Si surface in hexagonal pattern, then they coalesce to yield honeycomb cells [14]. However, at high oxygen pressure, the ablated particles are confined into gas phase, clusters and nanoparticles are formed, then stacked and coalesced onto the substrate. The nucleation is occurred into the gas phase rather than the substrate surface.

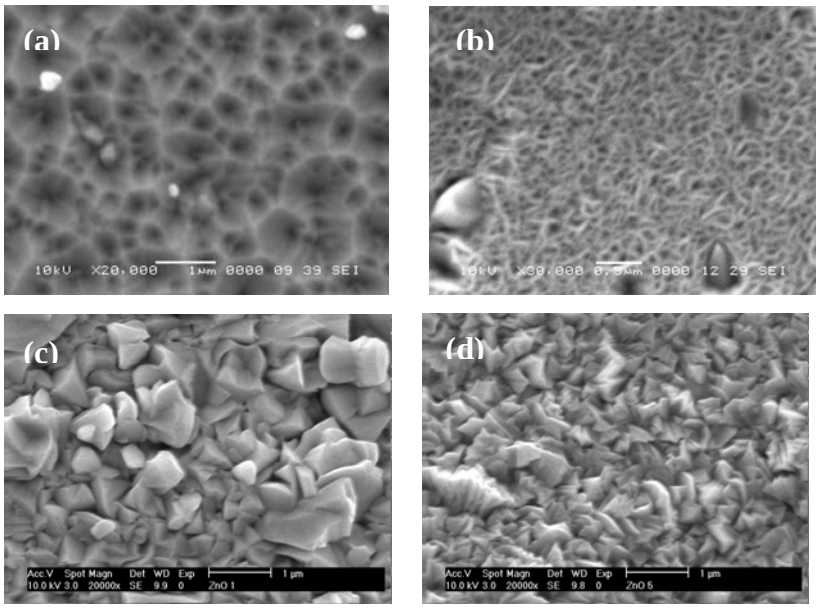

Figure 7: SEM surface micrographs of ZnO films carried out at different pressures on silicon substrate (a) 0.02, (b) 0.1, (c) 0.5 and (d) 5 *mbar*

Conclusion :

This work has been devoted to the ablation of ZnO target by a KrF excimer laser surrounding oxygen gas. Two dimensional evolution of plasma induced by laser ablation ZnO target under O_2 atmosphere was performed by ICCD camera. Plume spatio-temporal evolution was studied into vacuum and at different O_2 pressures from 10^{-2} to 10 *mbar*.

ICCD photography was revealed different phase during plasma expansion; plasma splitting, shock front formation, plasma front oscillation and Rayleigh Taylor instability apparition. These mechanisms are found to be strongly influenced by the background gas.

Furthermore, in order to identify plasma species, time integrated plasma emission spectrum has been investigated by optical emission spectroscopy diagnostic. Plasma emission spectrum shows the presence of Zn, Zn^+ and O emission lines both in vacuum and O_2 atmosphere. The emission intensity of Zn^+ line decreases as the distance from the target increases and disappears far from it. This could attribute to recombination process.

It was found that oxygen pressure affects directly the crystallinity and the morphology of ZnO films. At high oxygen pressure the films exhibit microcrystalline structure with random crystalline orientation. On the other hand, well oriented c-axis ZnO films are obtained at low pressure. The surface morphology shows different structures. At 0.02 and 0.1 *mbar* honeycomb and spaghetti-like structures were respectively obtained whereas at 0.5 and 5 *mbar* different size and shape crystallites were grown.

References

[1] S. Metev, in Pulsed Laser Deposition of Thin Films, D. B. Chrisney and G. K. Hubler,eds, John Wiley & Sons, New York (1994).

[2] B. L. Zhu, X. Z. Zhao, S. Xu, F. H. Su, G. H. Li, X. G. Wu, J. Wu, R. Wu, J. Liu, Japanese Journal of Applied Physics, **47,** 2225-2229 **(**2008).

[3] S. S. Harilal, J. Appl. Phys., **102**, 123306-(1-6) (2007).

[4] D. B. Geohegan, A. Puretzky, I. Ivanov, G. Eres, Z. Liu, D. Styers-Barnett, H. Hu, B. Zhao, H. Cui, C. Rouleau, S. Jesse, P. F. Britt, H. Christen, K. Xiao and P. Fleming, Photon-based Nanoscience and Nanobiotechnology, in: J.J. Dubowski and S. Tanev (Eds), Springer 205-223 (2006).

[5] R. K. Singh, A. Kumar, B. G. Patel and K. P. Subramanian, J. Appl. Phys., **101,** 103301-(1-9) (2007).

[6] S. Abdelli-Messaci, T. Kerdja, S. Lafane, S. Malek, Spectrochimica Acta Part B **64,** 968-973 (2009).

[7] S. Lafane, T. Kerdja, S. Abdelli-Messaci, S. Malek, M. Maaza, Appl. Phys. A, **98**, 374 (2010).

[8] A.V. Bulgakov and N. M. Bulkakova, J. Phys. D, Appl. Phys. **31,** 693-703 (1998).

[9] K. R. Chen, J. N. Leboeuf, R. F. Wood, D. B. Geohegan, J. M. Donato, C. L. Liu and A. A. Puretzky, App. Surf. Sci., **96-98,** 45-49 (1996).

[10] F. Claeyssens, A. Cheesman, S. J. Henley, M. N. R. Ashold, J. Appl. Phys. **92,** 6886-6894 (2002).

[11] Y. Kawaguchi, A. Narazaki, T. Sato, H. Niino and A. Yabe, App. Surf. Sci. **197-198,** 268-272 (2002).

[12] G. K. Hubler, in Pulsed Laser Deposition of Thin Films, D. B. Chrisney and G. K. Hubler,eds, John Wiley & Sons, New York.

[13] W. J. Li, E. W. Shi, W. Z. Zhong and Z.W. Yin, Journal of Crystal Growth, **203,** 186 (1999).

[14] Y. Ma , C P Wong, X. T. Zeng, T. Yu1, Y. Zhu and Z. X. Shen, J. Phys. D: Appl. Phys. **42,** 065417 (2009).